

# Novel insights into the genetic diversity of *Parafavella* based on mitochondrial CO1 sequences

Jae-Ho Jung<sup>1</sup>  | Ji Hye Moon<sup>1</sup> | Kyung-Min Park<sup>2</sup> | Sanghee Kim<sup>2</sup> |  
John R. Dolan<sup>3</sup> | Eun Jin Yang<sup>4</sup>

<sup>1</sup>Department of Biology, Gangneung-Wonju National University, Gangneung, South Korea

<sup>2</sup>Division of Polar Life Sciences, Korea Polar Research Institute, Incheon, South Korea

<sup>3</sup>CNRS UMR 7093, Laboratoire d'Océanographie de Villefranche-sur-Mer, Station Zoologique, Sorbonne Université, UPMC Univ Paris 06, Villefranche-sur-Mer, France

<sup>4</sup>Division of Polar Ocean Sciences, Korea Polar Research Institute, Incheon, South Korea

## Correspondence

Jae-Ho Jung, Department of Biology, Gangneung-Wonju National University, 7 Jukheon-gil, Gangneung, South Korea, 25457.

Email: jhjung@gwnu.ac.kr

## Funding information

Korea Polar Research Institute, Grant/Award Number: PE17900 and PM18040 & 20160245; National Research Foundation of Korea, Grant/Award Number: NRF-2017R1C1B5017183

## Abstract

We used both nuclear ribosomal genes (28S rDNA, 18S rDNA, 5.8S rDNA, internal transcribed spacer regions: ITS1, ITS2) and mitochondrial CO1 sequences to group or distinguish morphotypes of *Parafavella*, a problematic genus of tintinnid ciliates of the marine microzooplankton. We sequenced 30 single cells of *Parafavella* from the Bering Sea, the Greenland Sea, and the East/Japan Sea. Sequences were obtained from 4 morphotypes, typically ascribed to *P. gigantea*, *P. greenlandica*, *P. jorgenseni*, and *P. subrotundata* and from GenBank, the nuclear ribosomal genes of *P. parumdentata* were retrieved. Cells of the five morphotypes had identical 18S and 5.8S gene sequences. ITS1, ITS2 and 28S sequences produced two clusters: one grouping *P. greenlandica* and *P. parumdentata* and the other grouping *P. jorgenseni*, *P. gigantea*, and *P. subrotundata*. In contrast, CO1 nucleotide data yielded eight haplotypes clustered into five groups: one composed of *P. greenlandica* morphotypes, two distinct haplotypes of *P. jorgenseni*, and two distinct haplotypes of *P. gigantea* with one including *P. subrotundata* morphotypes. We investigated the co-occurrence of different morphotypes in samples from sites across a large gradient of latitude and concentrations of *Parafavella* cells. Natural communities contained 2–6 different morphotypes. We conclude that both crypticity and polymorphism characterize *Parafavella*, as known for other tintinnid genera.

## KEYWORDS

cryptic species, marine plankton, polymorphism, Tintinnidea

## 1 | INTRODUCTION

There is a great deal of interest in assessing boreal flora and fauna given the rapid changes that have already occurred and are anticipated to continue in high latitude ecosystems. In a recent report on arctic marine biodiversity, the chapter on plankton (Lovejoy et al., 2017) specifically points out the scarcity and need for species data on phytoplankton and heterotrophic protists of the microzooplankton. Here we report on some tintinnid species of the microzooplankton commonly found in waters of the Arctic Ocean as well as the North Pacific and North Atlantic Oceans, forms that

have long considered being “troublesome.” These are forms of the genus *Parafavella*. The trouble investigators have had is distinguishing morphotypes described as distinct species when intermediate forms appear to exist. This trouble has existed for some time now. Likely the first sceptic was Ostefeld (1910) reporting on the existence of morphologically intermediate forms between those described as “species” of *Parafavella* earlier by Brandt (1896). Later Schulz and Wulff (1927, 1929) in two large studies argued that there was but one species of *Parafavella* based on the variety of loricas found in the Barents Sea. Burkovsky (1973) postulated that lorica morphology of *Parafavella* changed seasonally

in the White Sea. Gold and Morales (1975) documented a large variability in empty *Parafavella* lorica. The last concerted attempts to cast doubt on lorica-morphology-based species boundaries in these common boreal tintinnids were studies by Davis concerning *Parafavella* (Davis, 1978). His remarks echoed those of earlier researchers; Davis stated “... I experienced many vexations in attempting the classification of specimens.” (Davis, 1978, p. 1823) Adding to the troubles and confusion of those attempting to put names on forms is the fact that in the classic monograph on tintinnid ciliates, Kofoid & Campbell, 1929, many of the illustrations are not drawn to the scale of the source illustrations (e.g., Supporting Information Figure S1 showing some *Parafavella* spp.). Thus, investigators may assign different names to the same morphotype depending on apparent relative sizes (with no indication of variability) as shown in Kofoid and Campbell (1929) or the dimensions (and notes on variability) given in the original descriptions.

In recent years, nuclear ribosomal genes have been applied to distinguish ciliate species and infer their phylogeny as DNA barcode (Pawlowski et al., 2012; Stoeck, Przybos, & Dunthorn, 2014). Ciliates are suspected to contain a huge species diversity considering estimates of the numbers of as yet undescribed species (Foissner, Chao, & Katz, 2008). An existing challenge is to separate closely related species efficiently using molecular methods. It has become apparent that 18S rDNA, one of most common genes for ciliate taxonomy/phylogeny, appears to have an insufficient resolution for species identification. For instance, the 18S rDNA is completely identical between some species of *Tetrahymena* (Lynn & Strüder-Kypke, 2006) and shows more than 99.9% genetic similarity between some congeners in *Pleurotricha* (Park, Moon, Kim, & Jung, 2017). Because of the problematic resolution, there have been efforts to establish new genetic marker as a barcode for ciliates (Barth, Krenek, Fokin, & Berendonk, 2006; Stoeck et al., 2014). For tintinnids, Santoferrara, McManus, and Alder (2013) assessed the nuclear genes as a potential barcoding tool, and Santoferrara et al. (2016) suggested a guideline for data collection and evaluation. In addition, Santoferrara, Tian, Alder, and McManus (2015) reported the crypticity and polymorphism in the genus *Helicostomella* based on the ribosomal genes.

As mentioned by Santoferrara et al. (2016), the mitochondrial cytochrome *c* oxidase subunit I (CO1) gene had not yet been amplified for the tintinnids. After the first report of intraspecific genetic variation using the CO1 in *Paramecium* (Barth et al., 2006), Strüder-Kypke and Lynn (2010) provided a primer pair, which successfully amplifies the CO1 from five ciliate classes. Considering its greater intraspecific variation than any nuclear genes, the CO1 can shed light on population genetics and biogeography. However, it should be noted that CO1 does not satisfy the CBOL (Consortium for the Barcode of Life)'s criteria as a barcode for all ciliates.

Stoeck et al. (2014) noted that some ciliates from anoxic habitats lack active mitochondria and CO1. Furthermore, not all ciliate CO1 can be amplified using the existing CO1 primers (e.g., Litostomatea, Spirotrichea). Rather than as a ciliate barcode, the CO1 can be utilized for the separation of closely related species or populations targeting specific ciliates. Park et al. (2018) provided a new primer pair, which can amplify the class Spirotrichea, and they successfully amplified *Tintinnopsis* cf. *cylindrica*. Here these new primers were applied to resolve the problematic situation among *Parafavella* forms.

To clarify the relationships among morphotypes of *Parafavella*, we employed single cell sequencing allowing us to investigate the genetic relationships of some more or less distinct morphotypes of *Parafavella*. We sequenced both nuclear ribosomal genes (28S rDNA, 18S rDNA, 5.8S rDNA, internal transcribed spacer regions: ITS1, ITS2) and as well as mitochondrial CO1 sequences to group or distinguish morphotypes of *Parafavella*. We also investigated the co-occurrence of the more or less distinct morphotypes in natural populations by examining material from sites sampled in a transect from the North Pacific into the High Arctic in the summer of 2017.

## 2 | MATERIALS AND METHODS

### 2.1 | Sampling

For the genetic analysis, plankton net-tow samples were obtained from three distinct seas using 20- $\mu$ m mesh plankton net (for details, see Figure 1; Table 1). The samples were fixed with neutral Lugol's solution (final concentration of 0.04% iodine [w/v]; 0.6% potassium iodide [w/v]) or ethanol (final concentration of 70%).

For the analysis of *Parafavella* forms found in natural assemblages of tintinnids, plankton net-tow samples (20-mesh plankton net) obtained from stations along a transect from the North Pacific (44°N) to the High Arctic (78°N) sampled in 2017 from aboard the Korean Icebreaker *Araon* were analysed. Net-tows sampled the water column from 100 m depth to the surface except at some shallow water stations. Aliquots of net-tow material for microscopic analysis were fixed with Lugol's Iodine (as above) solution.

### 2.2 | Morphology

For genetic analysis, individual cells were first isolated using a micro-capillary under a stereomicroscope (SZ11, Olympus, Japan), and micrographs were captured and measured under an inverted microscope (Eclipse Ti-U, Nikon, Japan) or standard microscopes (Zeiss Axio Imager 2 Carl Zeiss, Germany; BX53, Olympus, Japan) to record the morphology of the cells sequenced.

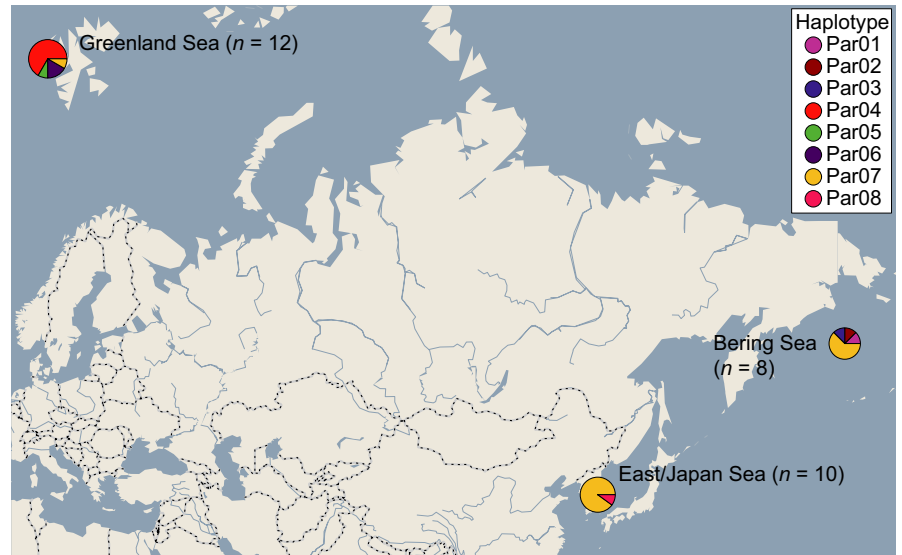


**FIGURE 1** Map of the locations sampled from three different seas. The numbers in parenthesis denote the number of specimens sequenced in this study. The haplotype represents CO1 nucleotide diversity [Colour figure can be viewed at [wileyonlinelibrary.com](http://wileyonlinelibrary.com)]

For analysis of the occurrence of forms of *Parafavella* in natural assemblages, aliquots of net tow material from the 2017 sampling were diluted and examined in 3-ml settling chambers. Material in the settling chambers was examined using an Olympus inverted microscope (IX71) equipped with differential interference contrast optics and an Olympus DP71 camera piloted using Olympus Biocell imaging software. Initially all tintinnids in a single aliquot were enumerated. For samples in which *Parafavella* were found (samples from nine stations), multiple aliquots were examined. For these latter samples, all *Parafavella* encountered which were correctly oriented for morphological diagnoses were photographed and multiple aliquots examined until a total of 20–30 cells from the sample were photographed. Only lorica containing a ciliate cell were recorded as empty lorica are not a reliable evidence of living cells (Dolan & Yang, 2017). *Parafavella* “species” identification (based upon lorica morphology) were made relying as much as possible on illustrations and dimensions as given in the original descriptions (for details see “*Parafavella* “species” designations—taxonomic notes” in the Supporting Information Appendix S1).

### 2.3 | DNA extraction, PCR and DNA sequencing

Each individual was transferred to 1.5 ml tube and its genomic DNA was extracted using RED-Extract-N-Amp Tissue PCR Kit (Sigma, St. Louis, MO, USA) according to the manufacturer’s instruction. Two PCRs were conducted to amplify nuclear ribosomal genes and mitochondrial CO1 gene. The conditions for the ribosomal genes were as follows: denaturation at 94°C for 1 min 30 s, followed by 40 cycles of denaturation at 98°C for 10 s, annealing at 58.5°C for 30 s and extension at 72°C for 3 min and a final extension step at 72°C for 7 min. The PCR product that covered the genes consisting of 18S rDNA, internal transcribed spacer

regions (ITS1, ITS2), 5.8S rDNA, and 28S rDNA (D1, D2) was amplified using slightly modified two primers (New Euk A and LSU rev2) that were described by Sonnenberg, Nolte, and Tautz (2007). DNA sequencing was performed using three additional internal primers (18SF790v2: 5’-AAA TTA KAG TGT TYM ARG CAG-3’ and 18SR300: 5’-CAT GGT AGT CCA ATA CAC TAC-3’, 18SF1470: 5’-TCT GTG ATG CCC TTA GAT GTC-3’) and an ABI 3700 sequencer (Applied Biosystems, Foster City, CA, USA). For the conditions of CO1, it was as follows: denaturation at 94°C for 1 min 30 s, followed by 40 cycles of denaturation at 98°C for 10 s, annealing at 53°C for 30 s and extension at 72°C for 1 min, and a final extension step at 72°C for 7 min (for details and primers, see Park et al., 2018). All PCR products were purified using a MEGAquick-spin Total Fragment DNA Purification Kit (iNtRON, Korea). Sequence fragments were assembled using Geneious 9.1.6 (Kearse et al., 2012).

### 2.4 | Molecular data analyses

To infer the phylogenetic position of the four tintinnid species, 18S rRNA gene sequences of 199 ciliates were retrieved from the NCBI database, including 197 tintinnids and two oligotrichs, *Novistrombidium orientale* (FJ422988) and *Strombidium stylifer* (DQ631805), as outgroups. The sequences were aligned using Muscle alignment (Edgar, 2004) in Geneious, and both ends of the alignment were manually trimmed using the Geneious. The best-fit model of substitution for phylogenetic analysis was selected using jModelTest 2.1.10 (Darriba, Taboada, Doallo, & Posada, 2012). We selected the model TIM2 + I (0.5690) + G (0.4550) for 18S rDNA and HKY + I (0.6480) for CO1 based on the Akaike information criterion (AIC). As an outgroup of CO1 tree, *Tintinnopsis* cf. *cylindrica* (MG594903) was selected. IQ-TREE 1.5.3

**TABLE 1** List of species analysed in this study with morphological and DNA sequences data

Species	Sampling data			Measurements			Ribosomal genes (18S–ITS1–5.8S–ITS2–28S, 2,945 bp)	COI gene (478 bp)
	Isolate	Date	Latitude/longitude	Lorica oral diameter	Length			
<i>P. jorgenseni</i>	Ara01	7/24/2012	N54°19'59.4"E173°39'58.8" (Bering Sea)	43.1	96.7		MH673380	MH673350
<i>P. jorgenseni</i>	Ara02	7/24/2012	N54°19'59.4"E173°39'58.8" (Bering Sea)	48.0	106.3		MH673381	MH673351
<i>P. jorgenseni</i>	Ara03	7/24/2012	N54°19'59.4"E173°39'58.8" (Bering Sea)	46.2	105.7		MH673382	MH673352
<i>P. subrotundata</i>	Ara04	7/26/2012	N58°45'10.2"W178°29'41.4" (Bering Sea)	60.6	250.8		MH673383	MH673353
<i>P. subrotundata</i>	Ara05	7/26/2012	N58°45'10.2"W178°29'41.4" (Bering Sea)	62.6	163.2		MH673384	MH673354
<i>P. subrotundata</i>	Ara06	7/26/2012	N58°45'10.2"W178°29'41.4" (Bering Sea)	63.4	186.8		MH673385	MH673355
<i>P. subrotundata</i>	Ara07	7/26/2012	N58°45'10.2"W178°29'41.4" (Bering Sea)	57.4	202.8		MH673386	MH673356
<i>P. gigantea</i>	Ara08	7/27/2012	N62°30'35.4"W173°59'54.0" (Bering Sea)	67.0	515.6		MH673387	MH673357
<i>P. gigantea</i>	Arc01	7/23/2017	N78°55'42.5"E11°56'18.5" (Greenland Sea)	59.0	399.8		MH673388	MH673358
<i>P. gigantea</i>	Arc02	7/23/2017	N78°55'42.5"E11°56'18.5" (Greenland Sea)	60.1	390.5		MH673389	MH673359
<i>P. gigantea</i>	Arc03	7/23/2017	N78°55'42.5"E11°56'18.5" (Greenland Sea)	62.9	415.0		MH673390	MH673360
<i>P. gigantea</i>	Arc04	7/23/2017	N78°55'42.5"E11°56'18.5" (Greenland Sea)	60.6	426.8		MH673391	MH673361
<i>P. gigantea</i>	Arc05	7/23/2017	N78°55'42.5"E11°56'18.5" (Greenland Sea)	61.6	366.0		MH673392	MH673362
<i>P. gigantea</i>	Arc06	7/23/2017	N78°55'42.5"E11°56'18.5" (Greenland Sea)	58.7	511.1		MH673393	MH673363
<i>P. gigantea</i>	Arc07	7/23/2017	N78°55'42.5"E11°56'18.5" (Greenland Sea)	49.3	360.4		MH673394	MH673364
<i>P. gigantea</i>	Arc08	7/23/2017	N78°55'42.5"E11°56'18.5" (Greenland Sea)	54.5	452.4		MH673395	MH673365
<i>P. gigantea</i>	Arc09	7/23/2017	N78°55'42.5"E11°56'18.5" (Greenland Sea)	58.2	419.1		MH673396	MH673366
<i>P. gigantea</i>	Arc10	7/23/2017	N78°55'42.5"E11°56'18.5" (Greenland Sea)	52.1	277.9		MH673397	MH673367
<i>P. greenlandica</i>	Arc11	7/14/2017	N78°55'40.9"E11°56'11.8" (Greenland Sea)	34.8	86.4		MH673398	MH673368
<i>P. greenlandica</i>	Arc12	7/14/2017	N78°55'40.9"E11°56'11.8" (Greenland Sea)	33.2	78.4		MH673399	MH673369
<i>P. gigantea</i>	Kor01	5/23/2016	N37°46'18.4"E128°57'5.6" (East/Japan Sea)	57.8	285.3		MH673400	MH673370
<i>P. gigantea</i>	Kor02	3/11/2016	N37°52'1.0"E128°50'54.4" (East/Japan Sea)	60.9	378.9		MH673401	MH673371
<i>P. gigantea</i>	Kor03	3/3/2016	N38°9'18.1"E128°36'34.1" (East/Japan Sea)	61.6	376.1		MH673402	MH673372
<i>P. gigantea</i>	Kor04	3/11/2016	N37°46'18.4"E128°57'5.6" (East/Japan Sea)	59.6	269.0		MH673403	MH673373
<i>P. gigantea</i>	Kor05	3/11/2016	N37°46'18.4"E128°57'5.6" (East/Japan Sea)	60.8	434.2		MH673404	MH673374
<i>P. gigantea</i>	Kor06	3/11/2016	N37°46'18.4"E128°57'5.6" (East/Japan Sea)	62.6	416.9		MH673405	MH673375
<i>P. gigantea</i>	Kor07	3/11/2016	N37°46'18.4"E128°57'5.6" (East/Japan Sea)	61.7	375.6		MH673406	MH673376
<i>P. gigantea</i>	Kor08	3/11/2016	N37°46'18.4"E128°57'5.6" (East/Japan Sea)	61.0	348.4		MH673407	MH673377
<i>P. gigantea</i>	Kor09	3/11/2016	N37°46'18.4"E128°57'5.6" (East/Japan Sea)	60.8	312.0		MH673408	MH673378
<i>P. gigantea</i>	Kor10	3/11/2016	N37°46'18.4"E128°57'5.6" (East/Japan Sea)	59.7	295.5		MH673409	MH673379

was used to render maximum-likelihood (ML) trees, with 1,000 bootstrap replicates (Nguyen, Schmidt, Haeseler, & Minh, 2015). A consensus ML tree was annotated using ggtree 1.8.2 in R (Yu, Smith, Zhu, Guan, & Lam, 2017). In addition, the tree using concatenated 28S rDNA, 5.8S rDNA and ITS regions was inferred with the best-fit model TrN + G (0.1040). *Laackmanniella prolongata* JQ924056 was selected as an outgroup. Uncorrected pairwise distances were measured using the Geneious.

To infer the median-joining network of CO1 haplotype, POPART 1.7 was used (Leigh & Bryant, 2015). Input file includes the CO1 nucleotide sequences with its sampling location (latitude, longitude) to plot them in a map. The program assigned the CO1 sequences into each haplotype and plotted in default map.

In R, the ggplot2 (Wickham, 2009) was used to plot the 30 specimens annotated with its CO1 haplotype and species name to examine the relationship between the haplotypes and morphology. To represent sequence difference matrices, eight sequence data sets were set up to discern a resolution of species identification for *Parafavella* and they were as follows: 18S rDNA (1,745 bp), ITS1 (101 bp), 5.8S (152 bp), ITS2 (194 bp), 28S (D1, D2; 753 bp), 28S (D1, D2; 594 bp, shorter than previous one to make the sequences correspond with the reference sequence *P. parumdentata*), CO1 nucleotide (478 bp) and CO1 amino acids (159 aa) sequences. The sequence difference matrices measured by the Geneious were used to construct heatmaps using lattice in R (Sarkar, 2008).

### 3 | RESULTS

#### 3.1 | Lorica morphology of sequenced specimens

Four morphotypes of *Parafavella* were collected from three distinct seas and here their lorica morphologies are described briefly (Figure 2; Table 1). See the Supporting Information Appendix S1 for further details on distinguishing the morphotypes encountered.

*Parafavella jorgenseni* was collected from Bering Sea. Three specimens were sequenced: Lorica conical with reticulate surface, denticulate tilted outward on oral rim, 43.1–48.0  $\mu\text{m}$  in lorica oral diameter (LOD), 96.7–106.3  $\mu\text{m}$  in length, aboral end sharply pointed.

*Parafavella gigantea* was collected from the Bering Sea, Greenland Sea and East/Japan Sea. Twenty-one specimens were sequenced: Lorica cylindrical/conical with reticulate surface, denticulate tilted outward on oral rim, 49.3–62.9  $\mu\text{m}$  in LOD, 269.0–511.1  $\mu\text{m}$  in length, aboral end pointed; in Bering and Greenland Sea specimens lorica usually cylindrical without indentation on oral rim, long cylindrical lorica with relatively shorter aboral end (vs. lorica more conical, aboral end longer with the indentation on oral rim in the East/Japan Sea specimens).

*Parafavella greenlandica* was collected from Greenland Sea. Two specimens were sequenced: Lorica conical with reticulate surface, denticulate tilted outward on oral rim, 33.2–34.8  $\mu\text{m}$  in LOD, 78.4–86.4  $\mu\text{m}$  in length, aboral end somewhat bluntly pointed.

*Parafavella subrotundata* was collected from Bering Sea. Four specimens were examined, and their morphology is as follows: Lorica cylindrical with reticulate surface and indentation on oral rim, denticulate tilted outward on oral rim, 57.4–63.4  $\mu\text{m}$  in LOD, 163.2–250.8  $\mu\text{m}$  in length, aboral end short and pointed; one of the examined specimens with aboral end being toward inside of lorica.

Two small morphotypes, *P. greenlandica* and *P. jorgenseni*, were easily separated from each other by the LOD (Table 1). In contrast, the other larger morphotypes, *P. gigantea* and *P. subrotundata*, share a similar size of LOD. In particular, *P. gigantea* was collected from all seas and they can be split into two morphotypes. The specimens from Bering and Greenland Sea usually have the largely cylindrical lorica without the indentation on oral rim, while the Korean population has the slightly conical lorica with the indentation on the oral rim. However, these characteristics are not distinct across whole specimens. See the specimens *P. gigantea* Arc07 and Arc09 had slightly conical lorica.

#### 3.2 | Nuclear ribosomal genes

A total of six data sets were analysed to examine genetic relationships of the five morphotypes including *P. parumdentata* retrieved from GenBank (Figure 3). 18S and 5.8S gene sequences for the five species were completely identical (Figure 4a; Supporting Information Figure S2). It should be noted that one nucleotide difference in 18S of *P. parumdentata* in Figure 3 denotes an ambiguous one (n).

ITS1 and 2 yielded two clusters based on one (1.0%) and five (2.6%) nucleotide differences, respectively (Figures 3 and 4b). The two clusters consist of *P. greenlandica* + *P. parumdentata* and *P. jorgenseni* + *P. gigantea* + *P. subrotundata*, that is the intra/inter-specific variations were 0% and 0%–2.6%, respectively.

28S data sets consist of two alignments because of the sequence length difference of *P. parumdentata*. The other sequences obtained newly here are longer than the *P. parumdentata* sequence in GenBank. Thus, the main differences between the data sets are the sequence length and the absence/presence of *P. parumdentata* and so “28S” includes 753 bp of 30 sequences and “28S trimmed” includes 594 bp of 31 sequences. Both data sets showed the same three clusters and these clusters are as follows: (a) *P. greenlandica* + *P. parumdentata*; (b) *P. gigantea* (Greenland Sea); (c) *P. gigantea* (Bering Sea, East/Japan Sea) + *P. subrotundata* + *P. jorgenseni*. The intra/inter-specific variations were 0%–0.1%

and 0%–1.9% for “28S,” and 0%–0.2% and 0%–2.4% for “28S trimmed.” The cluster 1, “*P. greenlandica* and *P. parumdentata*,” share completely identical nucleotide sequences except for the gap/deletion of a nucleotide in *P. parumdentata*. Except for the gap, this cluster differed at 12 (2.0%) and 13 (2.2%) nucleotide positions from *P. gigantea* (Greenland Sea) and *P. gigantea* (Bering Sea, East/Japan Sea) + *P. subrotundata* + *P. jorgenseni*, respectively. A single nucleotide of the cluster *P. gigantea* (Greenland Sea) differed from *P. gigantea*

(Bering Sea, East/Japan Sea) and *P. subrotundata* and *P. jorgenseni* (Figures 3 and 4b).

The data from concatenated 28S, 5.8S, ITS regions showed the same clusters as the 28S data set because the cluster *P. greenlandica* + *P. parumdentata* based on ITS regions was completely identical to one of the three clusters based on the concatenated data and the 5.8S sequences have no variations (Figure 4b). The three clusters from the concatenated did not reflect distinct geographical distribution.

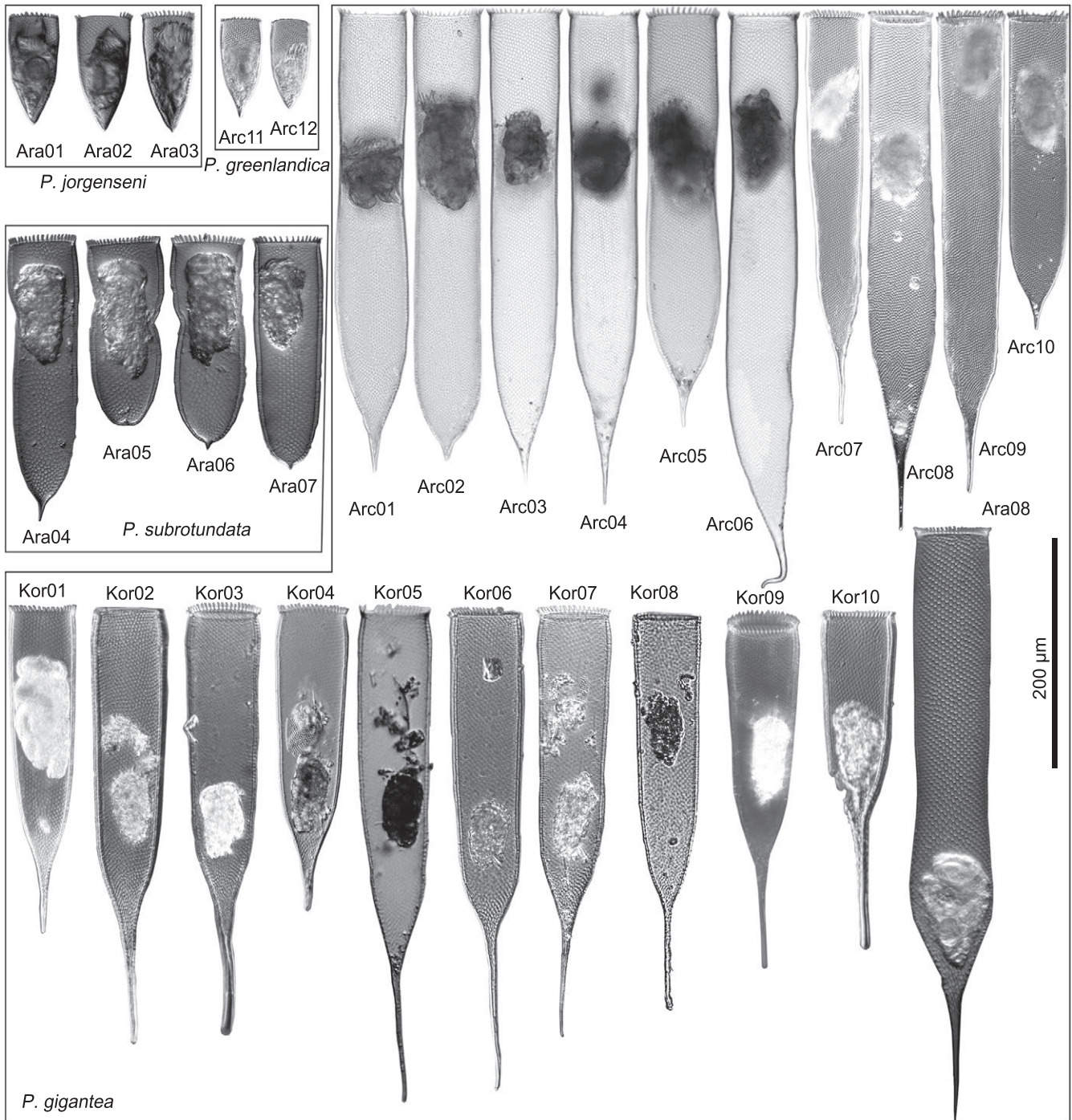


**FIGURE 2** Micrographs of four *Parafavella* species all at the same magnification

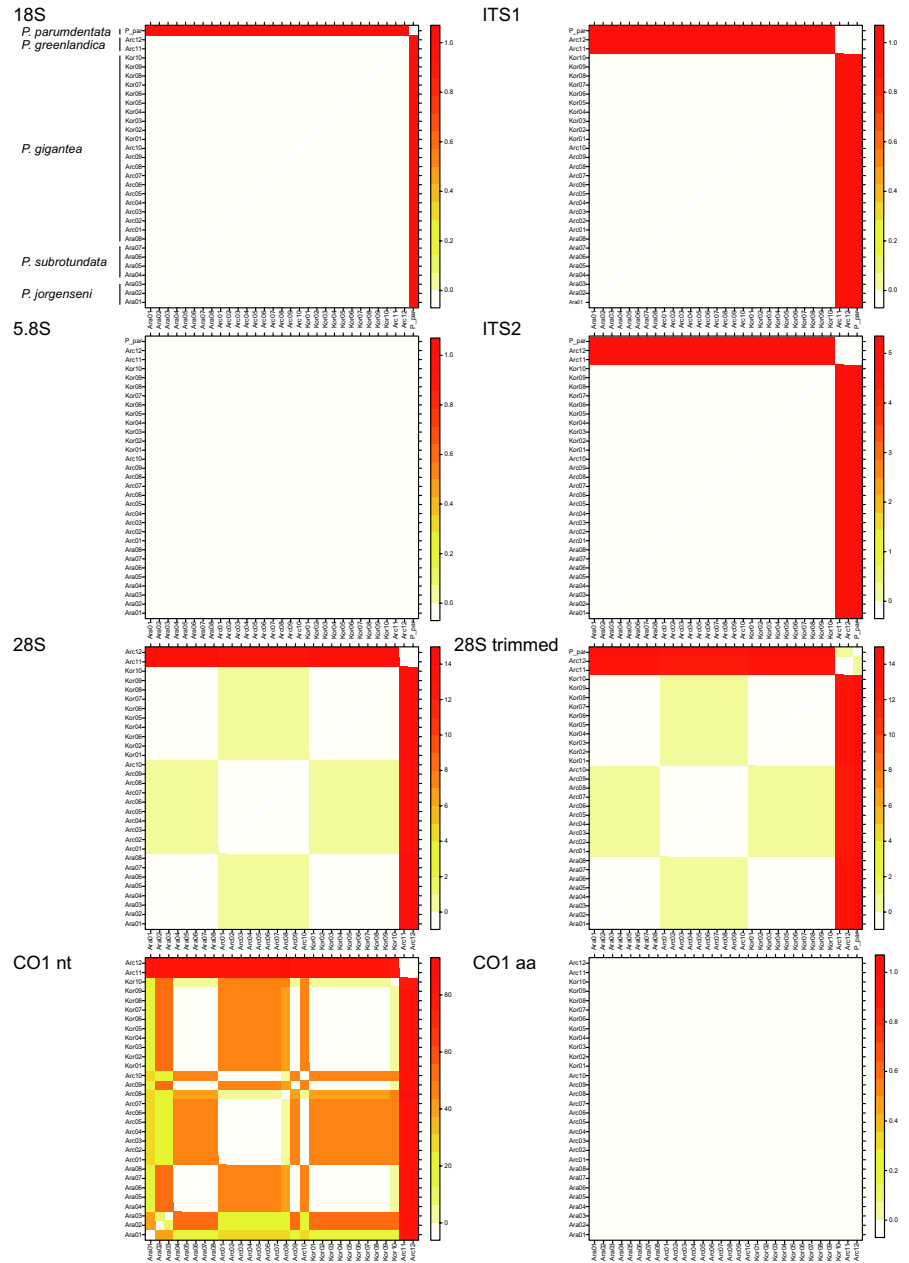


**FIGURE 3** Heatmaps based on genetic dissimilarities [Colour figure can be viewed at [wileyonlinelibrary.com](http://wileyonlinelibrary.com)]

### 3.3 | Mitochondrial CO1 gene

CO1 nucleotide data showed eight haplotypes while the amino acids set were all completely identical to each other (Figures 3 and 4c,d). Based on morphological identity, the intra/inter-specific variations of the nucleotide sequences were 0%–9.4% and 0%–18.2%, respectively. The CO1 nucleotide sequence of *Tintinnopsis* cf. *cylindrica* as an out-group showed inter-specific variations of 20.5%–23.4% while the amino acid sequence showed 1.3% from those of *Parafavella*.

*Parafavella gigantea* consisted of four haplotypes that clustered in two groups: (a) Par07 + Par08 and (b) Par04 + Par05. These two groups had 43–45 nucleotide differences (9.0%–9.4%) while each group had a single

nucleotide difference (0.2%) within them. The two sequences of *P. greenlandica* were completely identical and assigned to Par06. The three sequences of *P. jorgenseni* split into three haplotypes. Of these, Par02 showed nine (1.9%) nucleotide differences from Par03 while Par01 was highly distinct from Par02 + Par03 with 41 (8.6%) or 42 (8.8%) differences. Four sequences of *P. subrotundata* showed completely identical sequences with *P. gigantea* (East/Japan Sea) that assigned into Par07.

These eight haplotypes clustered into five groups based on the maximum likelihood tree and median-joining network using 97% similarity threshold (Figures 4 and 5): Par01 (*P. jorgenseni*); Par02 + Par03 (*P. jorgenseni*); Par04 + Par05 (*P. gigantea* from Greenland Sea); Par06 (*P. greenlandica*); and Par07 + Par08 (*P. gigantea* from all

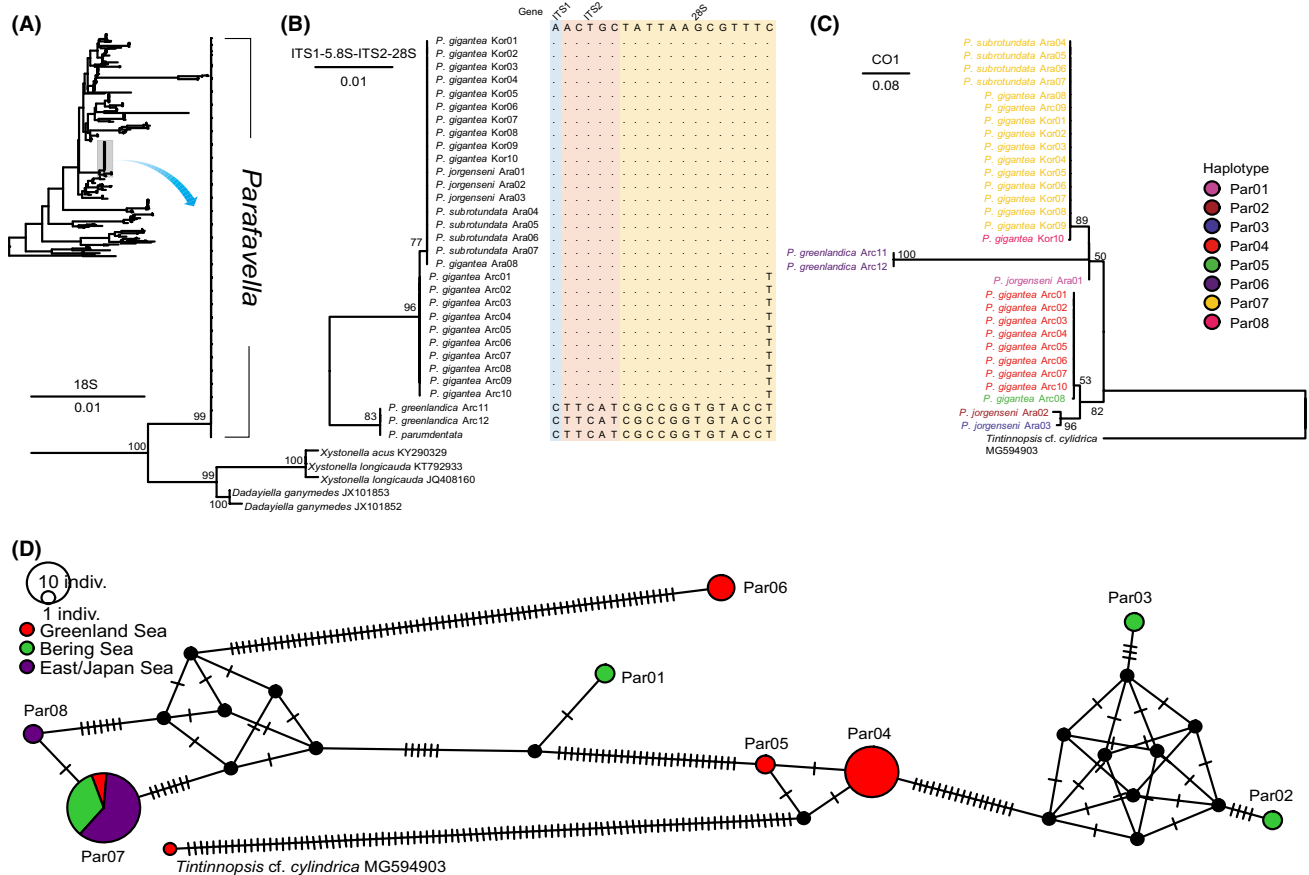


**FIGURE 4** Maximum-likelihood phylogenetic trees and median-joining network. The nucleotide matrix (b) denotes the variation in the concatenated 28S, 5.8S and ITS regions, and the network was constructed using CO1 nucleotide sequences [Colour figure can be viewed at [wileyonlinelibrary.com](http://wileyonlinelibrary.com)]

three seas and *P. subrotundata*). As shown above, the barcode gap between intra- and inter-specific variations was not observed.

### 3.4 | Biogeography of *Parafavella* based on genes

Of the nuclear ribosomal genes, 28S and ITS regions showed nucleotide variations only within and among *Parafavella* morphotypes (Figure 4b). One nucleotide difference was observed between the East/Japan Sea + the Bering Sea and the Greenland Sea for *P. gigantea*. The concatenated nucleotide sequences of *Parafavella* were completely identical within each population of the East/Japan and Bering Seas, respectively. Within the Greenland Sea population, two clusters were identified and each belongs to *P. greenlandica* and *P. gigantea* morphotype separated by 18 nucleotide differences.

Of the eight haplotypes in CO1, the Par07 was a common one and occurred from the all seas and groups *P. gigantea* with *P. subrotundata* (Figure 4d). The other haplotypes occurred only in one sea. Considering the number of haplotypes in each sea, the Greenland and Bering

Sea showed the highest number of haplotypes as four (vs. 2 and 1 in ribosomal genes), respectively. However, the East/Japan Sea was represented by just two haplotypes, which have only one nucleotide difference (vs. identical in ribosomal genes). It should be noted that the nuclear ribosomal genes were too conserved to allow discrimination among populations compared to the CO1 as expected (Figure 4b). However, the eight haplotypes clustering into five groups resulted in neither distinct biogeography nor gradient distribution pattern (Figure 4d). See Figure 4d, the eight haplotypes (or the five clusters), did not show certain biogeography among haplotypes/clusters.

### 3.5 | Co-occurrence of distinct *Parafavella* morphotypes in natural communities

*Parafavella* were found in nine samples from the 2017 cruise of the *Araon*. None contained only a single morphotype. The number of different *Parafavella* “species” (based on differences in the loricas) ranged from 2 to 6 within individual samples. Table 2 data suggest that there was no apparent relationship between the number of *Parafavella* morphotypes found and latitude. Nor was a relationship between with the

**TABLE 2** Numbers of different morphological species of *Parafavella* found in samples taken from the sites between the North Pacific and the Arctic in 2017. Note the wide range of natural communities sampled in terms of concentrations of *Parafavella* and total tintinnids ( $\sum$  tintinnids)

Station	Lat	Long	Date	<i>Parafavella</i> L <sup>-1</sup>	$\sum$ tintinnids L <sup>-1</sup>	Number of “spp”	Suppl plate
ARA08A01	42.3	151.2	7/27/2017	0.4	1.2	4	1. ARA08 St 1A
ARA08A03	46.6	159.4	7/29/2017	0.3	2.3	4	2. ARA08 St 3A
ARA08A04	48.9	163.5	7/29/2017	0.5	4.7	3	3. ARA08 St 4A
ARA08A05	51.1	167.6	7/29/2017	0.2	2.4	4	4. ARA08 St 5A
ARA08A06	53.1	171.6	7/30/2017	10.5	283.8	2	5. ARA08 St 6A
ARA08A07	55.1	175.7	7/31/2017	0.8	16.8	2	6. ARA08 St 7A
ARA08B02	66.6	-167.3	8/7/2017	10.2	165.6	6	7. ARA08 St 2B
ARA08B08	68.2	-166.9	8/7/2017	6.0	108.9	4	8. ARA08 St 8B
ARA08B21	77.7	180.0	8/15/2017	0.1	0.2	3	9. ARA08 St 21B

overall concentration of tintinnid ciliates or with the concentration of *Parafavella* cells and the number of morphotypes of *Parafavella* in a population (for details of the numbers and identities of *Parafavella* encountered, see the Supporting Information Plates 1–9).

## 4 | DISCUSSION

### 4.1 | Nuclear ribosomal genes

Previously, of all the species in *Parafavella*, nuclear gene data were available only for *P. parumdentata* (Santoferrara, Alder, & McManus, 2017). As in their 18S tree, here all five species of *Parafavella* including four species from this study clustered together because all sequences of *Parafavella* are completely identical with the exception of a single nucleotide in *P. parumdentata* (ambiguous nucleotide n) and showed a sister relationship with a cluster “*Dadayiella* + *Xystonella*.” Considering the five morphotypes in *Parafavella*, all nuclear ribosomal genes failed to distinguish among them. Even though the 28S showed three clusters, it is still less than the numbers of morphotypes (5) based on lorica morphology and the CO1 nucleotide haplotypes (8). Of the nuclear genes, the 28S has been considered as a useful barcoding tool for ciliates (Santoferrara et al., 2013; Stoeck et al., 2014). Santoferrara et al. (2013) separated tintinnids at 1% cut-off and Stoeck et al. (2014) identified that <0.6% sequence divergence was ideal to separate *Paramecium* species. If we follow these thresholds, only two clusters were identified as follows: cluster 1 containing *P. greenlandica* and *P. parumdentata* the other cluster containing *P. gigantea*, *P. subrotundata* and *P. jorgenseni*. Among tintinnids, *Helicostomella* is one of the best-known genera in terms of genetic data (Santoferrara et al., 2013, 2015; Xu, Sun, Shin, & Kim, 2012). According to Santoferrara et al. (2015), use of these multi-gene barcodes (i.e., 28S, 5.8S-ITS) is better than using a single gene to distinguish closely related species. However, we found that these

multi-genes performed little better than a single gene marker in *Parafavella* yielding only two clusters. Nonetheless we agree with the comment of Santoferrara et al. (2015) that because CO1 is much more variable than these nuclear genes it results in lower resolution at higher level of phylogeny (Park et al., 2018). In addition, genetic diversity of the CO1 can originate from heteroplasmy (i.e., intracellular polymorphism of mitochondrial genomes), nuclear encoded mitochondrial pseudogenes and hybrids (Tautz, Arctander, Minelli, Thomas, & Vogler, 2003; Zhao, Gentekaki, Yi, & Lin, 2013).

The recent development of high-throughput sequencing technology has focused on attention on the variable regions (i.e., V4) in 18S to capture eukaryote diversity (Filker, Gimmler, Dunthorn, Mahé, & Stoeck, 2015; Jung et al., 2015; Santoferrara, Rubin, & McManus, 2018; Stoeck et al., 2010). However, our data support the view that the nuclear ribosomal genes are of insufficient resolution below the genus level of *Parafavella* as shown in other tintinnids in previous reports (Santoferrara et al., 2013; Xu et al., 2012). In addition, there is evidence of low inter-specific variations in hypotrichs, benthic ciliates assigned to the ciliate class containing tintinnids (Park et al., 2017; Yi et al., 2008). Considering the 97%–98% similarity threshold commonly used by the high-throughput approaches for the species richness, it would appear that only a part of eukaryote diversity is unveiled at least with regard to ciliates.

### 4.2 | Mitochondrial CO1 gene

The CO1 of *Parafavella* was successfully amplified using the CO1 primers targeting spirotrichean ciliates (Park et al., 2018). Even though they provided only the CO1 of *Tintinnopsis* cf. *cylindrica* among tintinnids, our study suggests that other tintinnids could be sequenced using the primers. Strüder-Kypke and Lynn (2010) established new primers to amplify the CO1 of ciliates; however, as they mentioned,

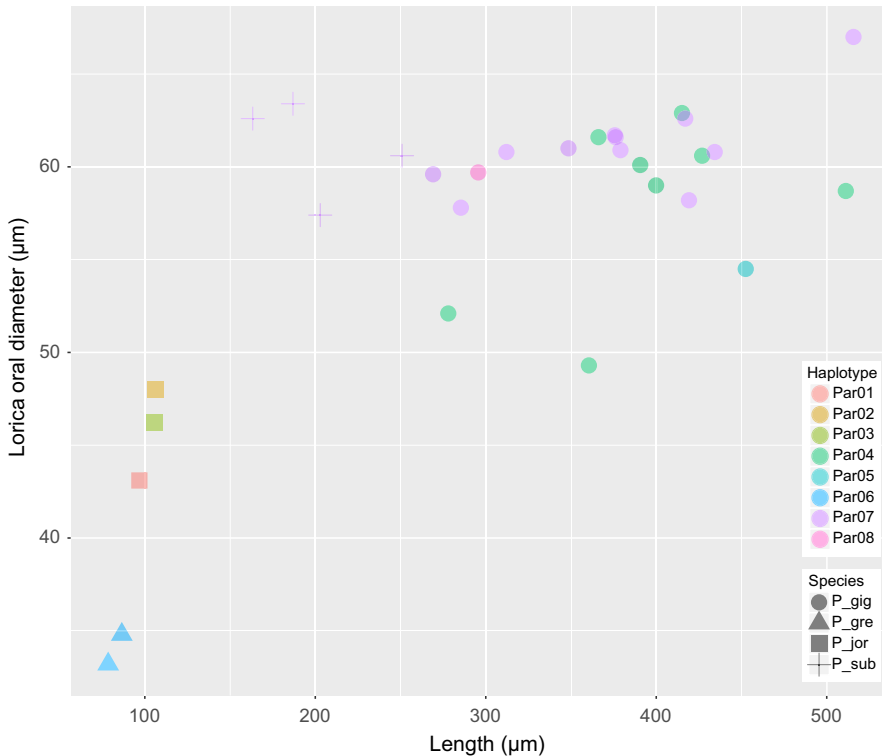


**FIGURE 5** Morphological characteristics and CO1 nucleotide haplotypes of four *Parafavella* species [Colour figure can be viewed at [wileyonlinelibrary.com](http://wileyonlinelibrary.com)]

they did not reliably amplify Litostomatea and Spirotrichea. The CO1 of *Parafavella* overlaps 260–348 bp with those regions from Strüder-Kypke and Lynn (2010). Across all sequences of *Parafavella*, none of indels occurred that resulted in frame shifts or be considered as nuclear encoded mitochondrial pseudogenes (Zhao et al., 2013).

The CO1 sequences of *Parafavella* showed higher genetic variation than the nuclear ribosomal genes, up to 18.2% in inter-specific variations. Considering the maximum of the inter-specific variations in the 28S, the CO1 showed the variations higher than seven times in *Parafavella*. A total of eight haplotypes were identified based on the CO1 nucleotide sequences that resulted in five clusters using 97% similarity threshold. If we follow the <1% intra-specific divergence as shown by Lynn and Strüder-Kypke (2006) and Chantangsi et al. (2007), six clusters can be identified because *P. jorgenseni* Ara02 and Ara03 have nine nucleotide differences between them (1.9%).

### 4.3 | Lorica morphology with CO1 haplotypes

The species designations of *Parafavella* have been contentious because of suspected lorica variability (Davis, 1978; Kofoid & Campbell, 1929; Schulz & Wulff, 1929). Kofoid and Campbell (1929) established the genus and assigned species status to 23 forms, most of which had been described originally as variants of other species. The most recent compendium of Zhang, Feng, Yu, Zhang, and Xiao (2012) lists

32 species found in the literature. In the WoRMS database (Warren, 2018), 35 species are listed including 6 as “taxon inquirendum,” suspected of being variants of other species.

Davis (1978) tried to distinguish *Parafavella* species collected from northern Norway waters; however, he failed to distinguish them based on lorica morphology alone. Even though some previous works considered them as a single polymorphic species (*P. denticulata*), he emphasized the need for further investigation of this genus using methods such as silver staining, electron microscopy, etc. Here, we found six clusters based the 1% cut-off value from the eight CO1 haplotypes. The results clearly showed that (a) *P. subrotundata* has identical nucleotide sequence with *P. gigantea*; (b) *P. gigantea* includes two clusters; (c) *P. jorgenseni* can be split into three clusters; and (d) *P. greenlandica* is distinct from the others.

*Parafavella subrotundata* collected from the Bering Sea showed completely identical sequences with *P. gigantea* in Par07, which is the most common haplotype across the three seas. Kofoid and Campbell (1929) considered that *P. subrotundata* “differs from *P. cylindrica* in stouter proportions and from *P. dilatata* in less conical bowl.” Based on our CO1 haplotypes, the results suggest that the cylindrical forms in *Parafavella* might be assigned to *P. gigantea*.

Of the specimens in our samples, we have *P. gigantea* with slightly posteriorly dilated lorica like *P. ventricosa* (see Arc02, Arc05, Arc08, Ara08). Even though the dilated form was not as distinct as shown in Kofoid and Campbell (1929), it suggests they might be conspecific.

Based on the tintinnids records reported in the Arctic Seas by Dolan, Pierce, and Yang (2017), *Parafavella denticulata* is the most commonly reported species in this genus. Even though we did not obtain the CO1 sequence from *P. denticulata*, it might be assigned to *P. gigantea* CO1 clusters like *P. subrotundata*.

Interestingly, the two species with short conical lorica, *P. greenlandica* and *P. jorgenseni*, did not cluster together and *P. greenlandica* was distinct from the other species in *Parafavella*. This finding suggests that the size and shape of the lorica are poor predictors of genetic relatedness in *Parafavella*. Considering the utility of oral denticulation in distinguishing species, we observed some *P. gigantea* with the denticulation, which was almost disconnected from the oral rim during the examination using the scanning electron microscopy (Supporting Information Figure S3). We also found *P. gigantea* without denticulation in Lugol's-fixed samples (see Supporting Information Plate 3 ARA08 St4A) in agreement with the observations of Davis (1978). Thus, oral denticulation does not appear to be reliable character among *Parafavella*. To date, data on the infraciliature of *Parafavella* are available only for *P. denticulata* and *P. gigantea* (Pierce, 1996). As mentioned by Santoferrara et al. (2016), infraciliature patterns can shed light on their biodiversity. Unfortunately, commercial production of protargol, the key chemical for protargol staining to examine infraciliature, has ended. We have tried to stain *Parafavella* using laboratory-synthesized protargol (Kim & Jung, 2017), but the stain quality was poor for the cells stored for a lengthy time in Bouin's solution. We recommend a focus on the infraciliature of representative haplotypes after screening the CO1 haplotypes rather than examining the infraciliature of all morphotypes.

#### 4.4 | Co-occurrence of distinct *Parafavella* morphotypes in natural communities

We found as many as six morphotypes, classically distinguished as distinct species, in a single sample. It is important to note that while many previous studies documented the co-occurrence of distinct lorica types of *Parafavella* (e.g., Ostefeld, 1910; Schulz & Wulff, 1927, 1929; Burkovsky, 1973; Davis, 1978) ours is the first study to rely solely on lorica containing ciliate cells. Empty tintinnid lorica are poor indicators of the occurrence and morphology of living tintinnids (Dolan & Yang, 2017; Kato & Taniguichi, 1993). However, it unclear what factors may influence the occurrence of distinct morphotypes of *Parafavella*. There was no obvious relationship between the number of morphotypes found and location in the form of latitude. Notably, there was no relationship between the number of morphotypes and either the concentration neither of *Parafavella* cells nor with concentrations of total tintinnids (Table 2).

Our findings with regard to the occurrence of *Parafavella* morphotypes contrast to findings with regard to *Cymatocylis* in Antarctic waters. Like *Parafavella* of boreal waters, Kim et al. (2013) found different morphotypes of *Cymatocylis* of the Southern Ocean microzooplankton, previously considered as distinct species, to be variants of a single species. The number of different morphotypes found in populations in the Amundsen Sea was unrelated to the concentration or composition of their phytoplankton prey but was positively related to the concentration of *Cymatocylis* cells (Dolan, Yang, Lee, & Kim, 2013). Culture work with *Favella* showed that lorica construction by a newly divided cell is rapid (2–10 min) and the length and shape of the lorica constructed appears to depend on the amount lorica material within the newly divided ciliate cell (reviewed in Agatha, Laval-Peuto, & M. Simon, P., 2013). It was then hypothesized that co-occurrence of multiple morphotypes of *Cymatocylis* reflected periods of rapid population growth with variable morphotypes formed by rapidly reproducing cells. This does not appear to be the case in *Parafavella*, as the number of morphotypes found in a population was not related to the concentration of *Parafavella*. At this time, we can offer no explanation for the apparent polymorphism of certain haplotypes of *Parafavella*.

#### ACKNOWLEDGEMENTS

This work was supported by grants from the National Research Foundation of Korea (NRF) funded by the Korea government (MSIP; Ministry of Science, ICT & Future Planning) (No. NRF-2017R1C1B5017183) and the Korea Polar Research Institute (KOPRI) (grant number PE17900). Partial support was provided by grants from the K-AOOS program (KOPRI; PM18040 & 20160245) funded by the MOF, Korea.

#### ORCID

Jae-Ho Jung  <http://orcid.org/0000-0001-5497-8678>

#### REFERENCES

- Agatha, S., Laval-Peuto, M., & Simon, P. (2013). The tintinnid lorica. In J. R. Dolan, S. Agatha, D. W. Coats, D. J. S. Montagnes, & D. K. Stocker (Eds.), *Biology and Ecology of tintinnid ciliates: Models for marine plankton* (pp. 17–41). Oxford, UK: Wiley-Blackwell.
- Barth, D., Krenek, S., Fokin, S. I., & Berendonk, T. U. (2006). Intraspecific genetic variation in *Paramecium* revealed by mitochondrial cytochrome *c* oxidase I sequences. *Journal of Eukaryotic Microbiology*, 53, 20–25. <https://doi.org/10.1111/j.1550-7408.2005.00068.x>
- Brandt, K. (1896). *Die Tintinnen*. *Bibliotheca Zoologica*, 20, 45–72.
- Burkovsky, I. V. (1973). Variability of *Parafavella denticulata* in the White Sea. *Zoologicheskii Zhurnal*, 52, 1277–1285.

- Chantangsi, C., Lynn, D. H., Brandl, M. T., Cole, J. C., Hetrick, N., & Ikononi, P. (2007). Barcoding ciliates: A comprehensive study of 75 isolates of the genus *Tetrahymena*. *International Journal of Systematic and Evolutionary Microbiology*, *57*, 2412–2425. <https://doi.org/10.1099/ijms.0.64865-0>
- Darriba, D., Taboada, G. L., Doallo, R., & Posada, D. (2012). jModelTest 2: More models, new heuristics and parallel computing. *Nature Methods*, *9*, 772. <https://doi.org/10.1038/nmeth.2109>
- Davis, C. C. (1978). Variations of the lorica in the genus *Parafavella* (Protozoa: Tintinnida) in northern Norway waters. *Canadian Journal of Zoology*, *56*, 1822–1827.
- Dolan, J. R., Pierce, R. W., & Yang, E. J. (2017). Tintinnid ciliates of the marine microzooplankton in Arctic Seas: A compilation and analysis of species records. *Polar Biology*, *40*, 1247–1260. <https://doi.org/10.1007/s00300-016-2049-0>
- Dolan, J. R., & Yang, E. J. (2017). Observations of apparent lorica variability in *Salpingacantha* (Ciliophora: Tintinnida) in the Northern Pacific and Arctic Oceans. *Acta Protozoologica*, *56*, 217–220.
- Dolan, J. R., Yang, E. J., Lee, S. H., & Kim, S. Y. (2013). Tintinnid ciliates of the Amundsen Sea (Antarctica) Plankton Communities. *Polar Research*, *32*, 19784.
- Edgar, R. C. (2004). MUSCLE: Multiple sequence alignment with high accuracy and high throughput. *Nucleic Acids Research*, *32*, 1792–1797. <https://doi.org/10.1093/nar/gkh340>
- Filker, S., Gimmler, A., Dunthorn, M., Mahé, F., & Stoeck, T. (2015). Deep sequencing uncovers protistan plankton diversity in the Portuguese Ria Formosa solar saltern ponds. *Extremophiles*, *19*, 283–295. <https://doi.org/10.1007/s00792-014-0713-2>
- Foissner, W., Chao, A., & Katz, L. A. (2008). Diversity and geographic distribution of ciliates (Protista: Ciliophora). *Biodiversity and Conservation*, *17*, 345–363. <https://doi.org/10.1007/s10531-007-9254-7>
- Gold, K., & Morales, E. A. (1975). Tintinnida of the New York Bight: Loricae of *Parafavella gigantea*, *P. parudentata*, and *Ptychocylis obtusa*. *Transactions of the American Microscopical Society*, *94*, 142–145.
- Jung, J.-H., Park, K.-M., Yang, E. J., Joo, H. M., Jeon, M., Kang, S.-H., ... Kim, S. (2015). Patchy-distributed ciliate (Protozoa) diversity of eight polar communities as determined by 454 amplicon pyrosequencing. *Animal Cells and Systems*, *19*, 339–349. <https://doi.org/10.1080/19768354.2015.1082931>
- Kato, S., & Taniguchi, A. (1993). Tintinnid ciliates as indicator species of different water masses in the western North Pacific Polar Front. *Fisheries Oceanography*, *2*, 166–174. <https://doi.org/10.1111/j.1365-2419.1993.tb00132.x>
- Kearse, M., Moir, R., Wilson, A., Stones-Havas, S., Cheung, M., Sturrock, S., ... Drummond, A. (2012). Geneious Basic: An integrated and extendable desktop software platform for the organization and analysis of sequence data. *Bioinformatics*, *28*, 1647–1649. <https://doi.org/10.1093/bioinformatics/bts199>
- Kim, S. Y., Choi, J. K., Dolan, J. R., Shin, H. C., Lee, S., & Yang, E. J. (2013). Morphological and ribosomal DNA-based characterization of six Antarctic ciliate 5 morphospecies from the Amundsen Sea with phylogenetic analyses. *Journal of Eukaryotic Microbiology*, *60*, 497–513.
- Kim, J. H., & Jung, J.-H. (2017). Cytological staining of protozoa: A case study on the impregnation of hypotrichs (Ciliophora: Spirotrichea) using laboratory-synthesized protargol. *Animal Cells and Systems*, *21*, 412–418. <https://doi.org/10.1080/19768354.2017.1376707>
- Kofoed, C. A., & Campbell, A. S. (1929). A conspectus of the marine and freshwater Ciliata belonging to the suborder Tintinninoidea, with descriptions of new species principally from the AGASSIZ expedition to the eastern tropical Pacific, 1904–1905. *University of California Publications in Zoology*, *34*, 1–403.
- Leigh, J. W., & Bryant, D. (2015). POPART: Full-feature software for haplotype network construction. *Methods in Ecology and Evolution*, *6*, 1110–1116.
- Lovejoy, C., von Quillfeldt, C., Hopcroft, R. R., Poulin, M., Mary Thaler, M., Arendt, K., ... Kosobokova, K. (2017). *Plankton in CAFF. 2017. State of the Arctic marine biodiversity: Key findings and advice for monitoring. conservation of Arctic flora and fauna*. Akureyri, Iceland: International Secretariat. ISBN 978-9935-431-62-2 (Retrieved from [www.arcticbiodiversity.is/marine](http://www.arcticbiodiversity.is/marine)).
- Lynn, D. H., & Strüder-Kypke, M. C. (2006). Species of *Tetrahymena* identical by small subunit rRNA gene sequences are discriminated by mitochondrial cytochrome *c* oxidase I gene sequences. *Journal of Eukaryotic Microbiology*, *53*, 385–387. <https://doi.org/10.1111/j.1550-7408.2006.00116.x>
- Nguyen, L.-T., Schmidt, H. A., von Haeseler, A., & Minh, B. Q. (2015). IQ-TREE: A fast and effective stochastic algorithm for estimating maximum-likelihood phylogenies. *Molecular Biology and Evolution*, *32*, 268–274. <https://doi.org/10.1093/molbev/msu300>
- Ostenfeld, C. H. (1910). Marine plankton from the East-Greenland Sea (W. of 6° W. long. and N. of 73°30' N. lat.) collected during the Danmark Expedition 1906–1908: II Protozoa. *Danmark-Ekspeditionen Til Gronlands Nordostkyst 1906–1908*, *3*, 287–300.
- Park, M.-H., Jung, J.-H., Jo, E., Park, K.-M., Baek, Y.-S., Kim, S.-J., & Min, G.-S. (2018). Utility of mitochondrial CO1 sequences for species discrimination of Spirotrichea ciliates (Protozoa, Ciliophora). *Mitochondrial DNA Part A*. <https://doi.org/10.1080/24701394.2018.1464563>
- Park, M.-H., Moon, J. H., Kim, K. N., & Jung, J.-H. (2017). Morphology, morphogenesis, and molecular phylogeny of *Pleurotricha oligocirrata* nov. spec. (Ciliophora: Spirotrichea: Stylonychinae). *European Journal of Protistology*, *59*, 114–123.
- Pawlowski, J., Audic, S., Adl, S., Bass, D., Belbahri, L., Berney, C., ... de Vargas, C. (2012). CBOL protist working group: Barcoding eukaryotic richness beyond the animal, plant, and fungal kingdoms. *PLoS Biology*, *10*, e1001419. <https://doi.org/10.1371/journal.pbio.1001419>
- Pierce, R. W. (1996). Morphology and infraciliature of selected species of Tintinnina with a phylogenetic analysis of the Tintinnina based on infraciliature. Dissertation, University of Rhode Island, Rhode Island, USA.
- Santoferrara, L. F., Alder, V. V., & McManus, G. B. (2017). Phylogeny, classification and diversity of Choreotrichia and Oligotrichia (Ciliophora, Spirotrichea). *Molecular Phylogenetics and Evolution*, *112*, 12–22. <https://doi.org/10.1016/j.ympev.2017.03.010>
- Santoferrara, L. F., Bachy, C., Alder, V. A., Gong, J., Kim, Y.-O., Saccà, A., ... Agatha, S. (2016). Updating biodiversity studies in loricate protists: The case of the tintinnids (Alveolata, Ciliophora, Spirotrichea). *Journal of Eukaryotic Microbiology*, *63*, 651–656. <https://doi.org/10.1111/jeu.12303>
- Santoferrara, L. F., McManus, G. B., & Alder, V. A. (2013). Utility of genetic markers and morphology for species discrimination within the order Tintinnida (Ciliophora, Spirotrichea). *Protist*, *164*, 24–36. <https://doi.org/10.1016/j.protis.2011.12.002>

- Santoferrara, L. F., Rubin, E., & McManus, G. B. (2018). Global and local DNA (meta)barcoding reveal new biogeography patterns in tintinnid ciliates. *Journal of Plankton Research*, 000, 000–000. <https://doi.org/10.1093/plankt/fby011>.
- Santoferrara, L. F., Tian, M., Alder, V. A., & McManus, G. B. (2015). Discrimination of closely related species in tintinnid ciliates: New insights on crypticity and polymorphism in the genus *Helicostomella*. *Protist*, 166, 78–92. <https://doi.org/10.1016/j.protis.2014.11.005>
- Sarkar, D. (2008). *Lattice: Multivariate data visualization with R*. New York: Springer.
- Schulz, B., & Wulff, A. (1927). Hydrographische und planktologische Ergebnisse der Fahrt des Fischereischutzbootes “Zeiten” in das Barentsmeer im August-September 1926. *Die Berichte Der Deutschen Wissenschaftlichen Kommission Für Meeresforschung*, 3, 211–280.
- Schulz, B., & Wulff, A. (1929). Hydrographie und Oberflächenplankton des Westlichen Barentsmeeres im Sommer 1927. *Ber Deutsch Wissensch Komm Meeresforsch*, 4, 7–141.
- Sonnenberg, R., Nolte, A. W., & Tautz, D. (2007). An evaluation of LSU rDNA D1–D2 sequences for their use in species identification. *Frontiers in Zoology*, 4, 6.
- Stoeck, T., Bass, D., Nebel, M., Christen, R., Jones, M. D. M., Breiner, H.-W., & Richards, T. A. (2010). Multiple marker parallel tag environmental DNA sequencing reveals a highly complex eukaryotic community in marine anoxic water. *Molecular Ecology*, 19, 21–31. <https://doi.org/10.1111/j.1365-294X.2009.04480.x>
- Stoeck, T., Przybos, E., & Dunthorn, M. (2014). The D1–D2 region of the large subunit ribosomal DNA as barcode for ciliates. *Molecular Ecology Resources*, 14, 458–468. <https://doi.org/10.1111/1755-0998.12195>
- Strüder-Kypke, M. C., & Lynn, D. H. (2010). Comparative analysis of the mitochondrial cytochrome *c* oxidase subunit I (COI) gene in ciliates (Alveolata, Ciliophora) and evaluation of its suitability as a biodiversity marker. *Systematics and Biodiversity*, 8, 131–148.
- Tautz, D., Arctander, P., Minelli, A., Thomas, R. H., & Vogler, A. P. (2003). A plea for DNA taxonomy. *Trends in Ecology & Evolution*, 18, 70–74. [https://doi.org/10.1016/S0169-5347\(02\)00041-1](https://doi.org/10.1016/S0169-5347(02)00041-1)
- Warren, A. (2018). World Ciliophora Database. Parafavella Kofoid & Campbell, 1929. Accessed through: World Register of Marine Species. Available at <https://www.marinespecies.org/aphia.php?p=taxdetails&xml:id=196836> (Accessed on 2018-05-01).
- Wickham, H. (2009). *ggplot2: Elegant Graphics for Data Analysis*. New York, NY: Springer-Verlag.
- Xu, D., Sun, P., Shin, M. K., & Kim, Y. O. (2012). Species boundaries in tintinnid ciliates: A case study – morphometric variability, molecular characterization, and temporal distribution of *Helicostomella* species (Ciliophora, Tintinnina). *Journal of Eukaryotic Microbiology*, 59, 351–358. <https://doi.org/10.1111/j.1550-7408.2012.00625.x>
- Yi, Z., Chen, Z., Warren, A., Roberts, D., Al-Rasheid, K., Miao, M., ... Song, W. (2008). Molecular phylogeny of *Pseudokeronopsis* (Protozoa, Ciliophora, Urostylida), with reconsideration of three closely related species at inter- and intra-specific levels inferred from the small subunit ribosomal RNA gene and the ITS1-5.8 S-ITS2 region sequences. *Journal of Zoology*, 275, 268–275.
- Yu, G., Smith, D. K., Zhu, H., Guan, Y., & Lam, T.-T.-Y. (2017). ggtree: An R package for visualization and annotation of phylogenetic trees with their covariates and other associated data. *Methods in Ecology and Evolution*, 8, 28–36.
- Zhang, W., Feng, M., Yu, Y., Zhang, C., & Xiao, T. (2012). *An illustrated guide to contemporary tintinnids in the world*. Beijing: Science Press.
- Zhao, Y., Gentekaki, E., Yi, Z., & Lin, X. (2013). Genetic differentiation of the mitochondrial cytochrome oxidase *c* subunit I gene in genus *Paramecium* (Protista, Ciliophora). *PLoS ONE*, 8, e77044. <https://doi.org/10.1371/journal.pone.0077044>

## SUPPORTING INFORMATION

Additional supporting information may be found online in the Supporting Information section at the end of the article.

**How to cite this article:** Jung J-H, Moon JH, Park K-M, Kim S, Dolan JR, Yang EJ. Novel insights into the genetic diversity of *Parafavella* based on mitochondrial CO1 sequences. *Zool Scr*. 2018;47:743–755. <https://doi.org/10.1111/zsc.12312>